Supplementary Information

The Influence of Different Ammonium Cations on the Optical Properties of Tetrakis Gd^{III} and Eu^{III} Complexes

Renata D. Adati, ****,a,b*** ***Jorge H. S. K. Monteiro,[a] Lucas P. Cardoso,[b] Daniel H. de Oliveira,[b] Miguel Jafelicci Jr.[a] and Marian R. Davolos*,[a]***

[a]Laboratório de Materiais Luminescentes, Departamento de Química Geral e Inorgânica, Instituto de Química, Universidade Estadual Paulista (Unesp), 14800-060 Araraquara-SP, Brazil

[b]Departamento de Química e Biologia, Universidade Tecnológica Federal do Paraná (UTFPR), 81280-340 Curitiba-PR, Brazil

Table S1. Infrared frequencies (wavenumber) for the tta ligand and the $Q^{+}[Eu(tta)_4]^{-}$ complexes

Compound	ν(C−H) / cm^{-1}	ν_a(C=O) / cm^{-1}	ν_s(C=O) / cm^{-1}	ν(C=C) / cm^{-1}	ν(C−O) / cm^{-1}	ν_s(C−F) / cm^{-1}
tta	3720-2289	1691	1632	1541	1353	1295
$(N(C_2H_5)_4)^{+}[Eu(tta)_4]^{-}$	2989	–	1605	1535 1507 1481	1356	1183 1133
$(N(C_4H_9)_4)^{+}[Eu(tta)_4]^{-}$	2967 2878	–	1606	1535 1504 1480	1356	1183 1133
$(N(C_{12}H_{25})_2(CH_3)_2)^{+}[Eu(tta)_4]^{-}$	2956	–	1616	1540	1356	1308

tta: 2-thenoyltrifluoracetone; bmdm: 1-(4-*tert*-butylphenyl)-3-(4-methoxyphenyl)propane-1,3-dione.

Table S2. Infrared frequencies for the bmdm ligand and the $Q^{+}[Eu(bmdm)_4]^{-}$ complexes

Compound	ν(C−H) / cm^{-1}	ν_a(C=O) / cm^{-1}	ν_s(C=O) / cm^{-1}	ν(C=C) / cm^{-1}	ν(C−O) / cm^{-1}	ν_a(C−O−C) / cm^{-1}
bmdm	3178 2950	1612	1586	1500	1353	1259 1182
$(N(C_2H_5)_4)^{+}[Eu(bmdm)_4]^{-}$	3238 2960	1594	1569	1527 1488 1434 1431 1461	1356	1254 1171
$(N(C_4H_9)_4)^{+}[Eu(bmdm)_4]^{-}$	3238 2960	1594	1569	1439 1458	1356	1254 1171
$(N(C_{12}H_{25})_2(CH_3)_2)^{+}[Eu(bmdm)_4]^{-}$	3238 2960	1594	1569	1439 1458	1356	1254 1171

tta: 2-thenoyltrifluoracetone; bmdm: 1-(4-*tert*-butylphenyl)-3-(4-methoxyphenyl)propane-1,3-dione.

*e-mail: renataadati@utfpr.edu.br; davolos@iq.unesp.br

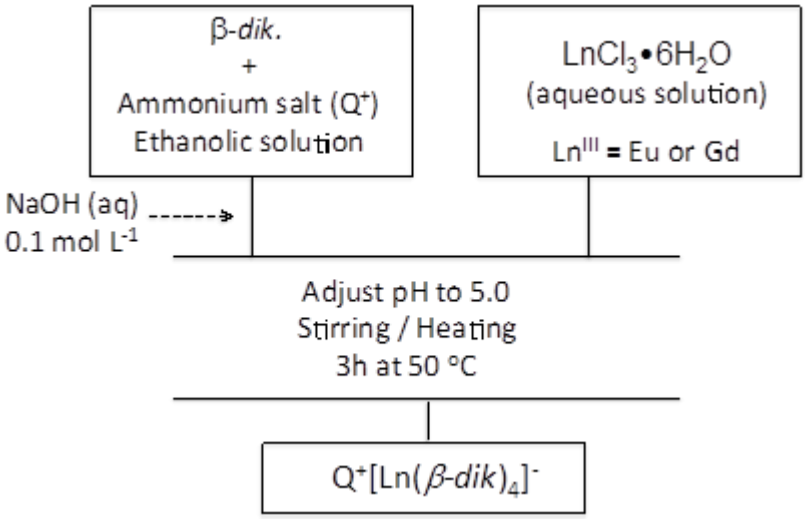

Figure S1. Synthetic route to the obtention of $Q^{+}[Ln(\beta\text{-dik})_4]^{-}$.

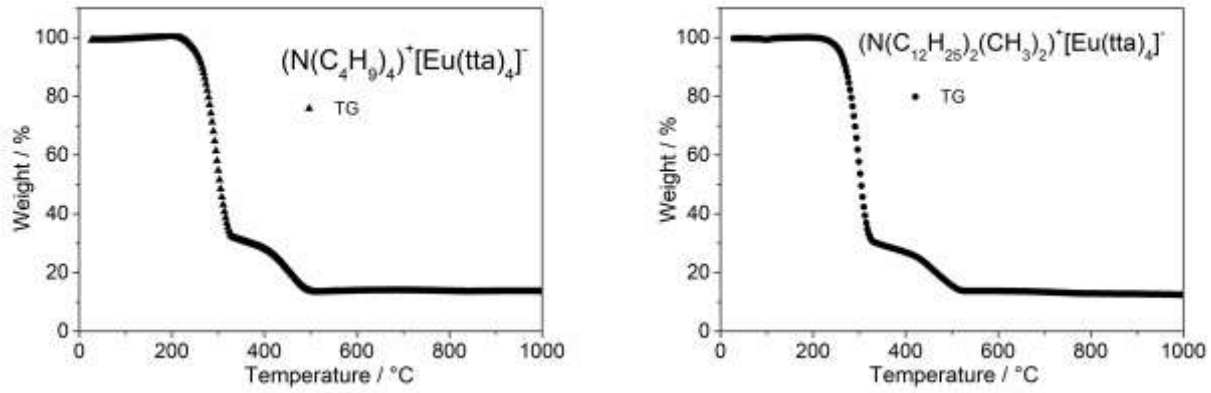

(a) (b)

Figure S2. TG curves of (a) $(N(C_4H_9)_4)^{+}[Eu(tta)_4]^{-}$ and (b) $(N(C_{12}H_{25})_2(CH_3)_2)^{+}[Eu(tta)_4]^{-}$ complexes.

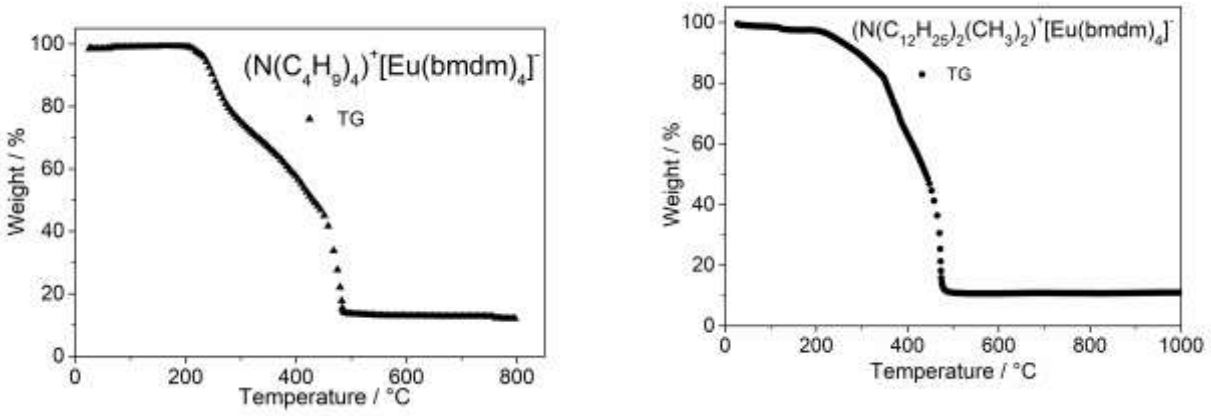

(a) (b)

Figure S3. TG curves of (a) $(N(C_4H_9)_4)^{+}[Eu(bmdm)_4]^{-}$ and (b) $(N(C_{12}H_{25})_2(CH_3)_2)^{+}[Eu(bmdm)_4]^{-}$ complexes.

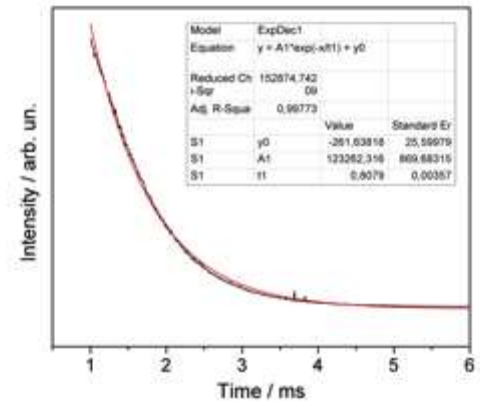

(a)

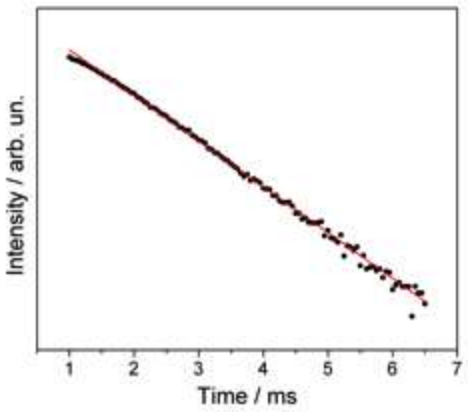

(b)

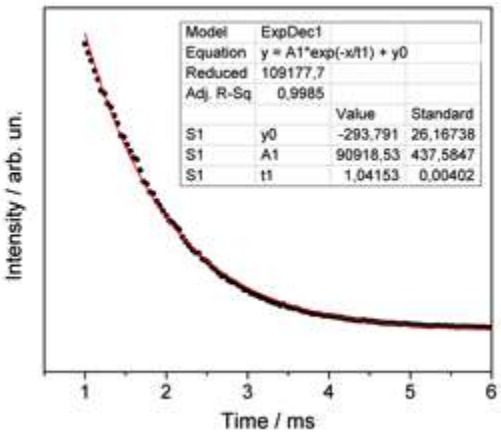

(c)

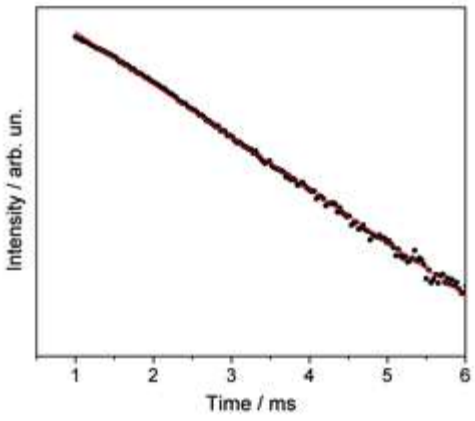

(d)

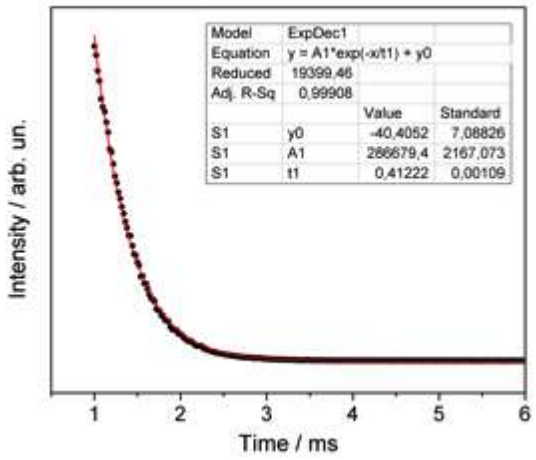

(e)

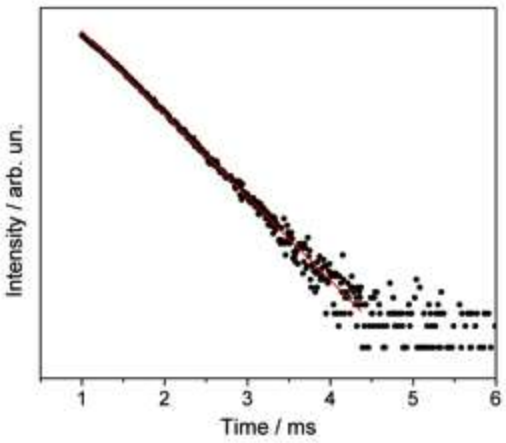

(f)

Figure S4. Emission decay curves and linearization for $Q^{+}[Eu(tta)_4]^{-}$. (a, b) Q = $(N(C_2H_5)_4)^{+}$; (c, d) Q = $(N(C_4H_9)_4)^{+}$; (e, f) Q = $(N(C_{12}H_{25})_2(CH_3)_2)^{+}$.

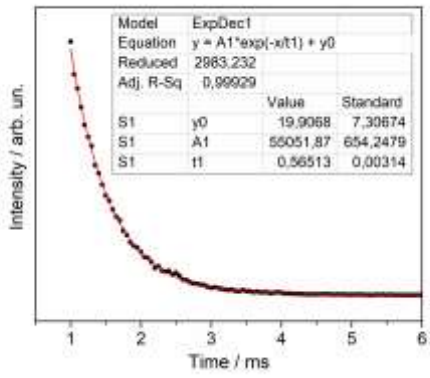

(a)

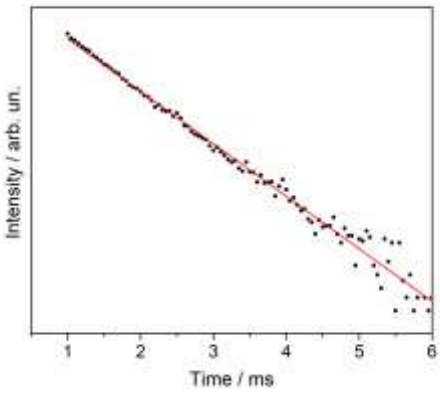

(b)

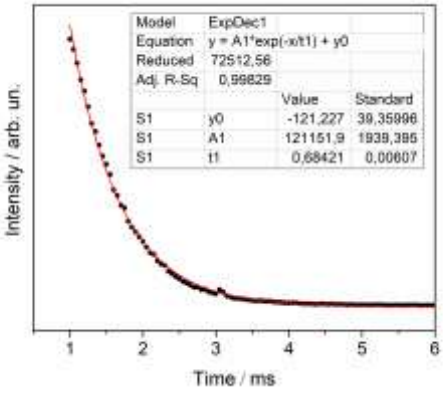

(c)

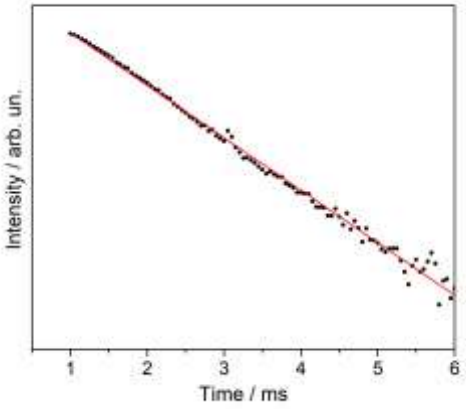

(d)

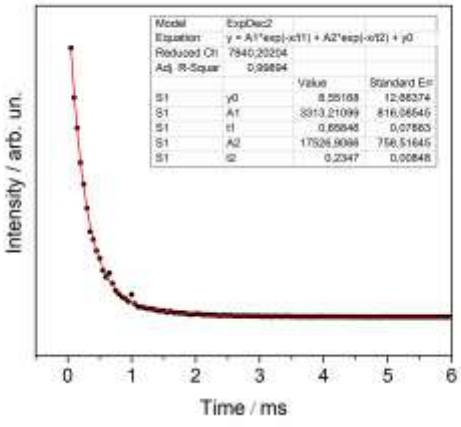

(e)

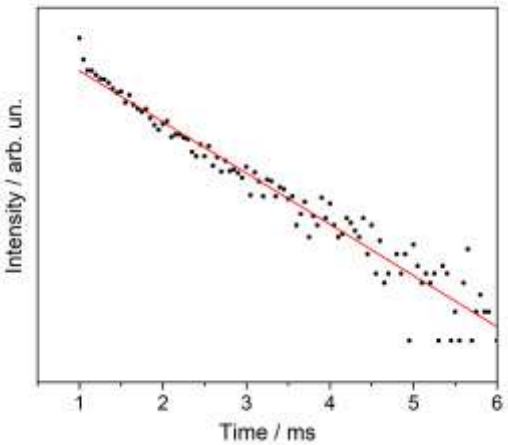

(f)

Figure S5. Emission decay curves and linearization for $Q^{+}[Eu(bmdm)_4]^{-}$. (a, b) Q = $(N(C_2H_5)_4)^{+}$; (c, d) Q = $(N(C_4H_9)_4)^{+}$; (e, f) Q = $(N(C_{12}H_{25})_2(CH_3)_2)^{+}$.

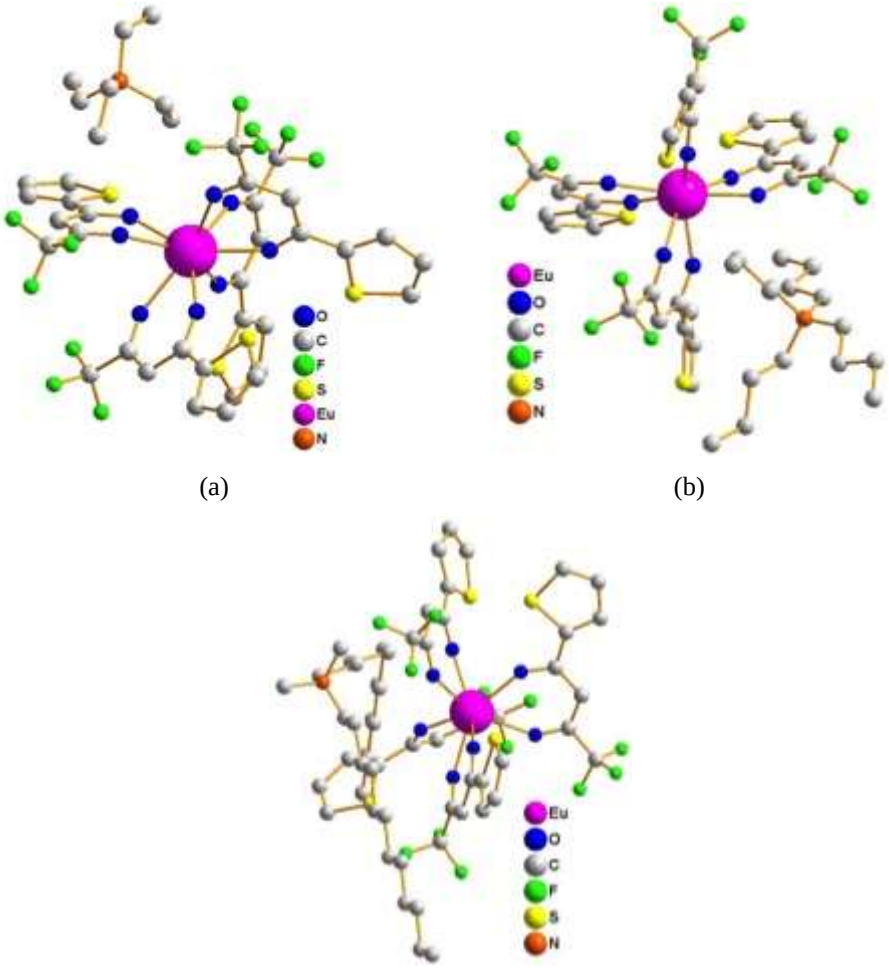

Figure S6. Ground state geometry of the (a) $(N(C_2H_5)_4)^+[Eu(tta)_4]^-$; (b) $(N(C_4H_9)_4)^+[Eu(tta)_4]^-$ and (c) $(N(C_{12}H_{25})_2(CH_3)_2)^+[Eu(tta)_4]^-$ complexes obtained by the Sparkle/PM6.

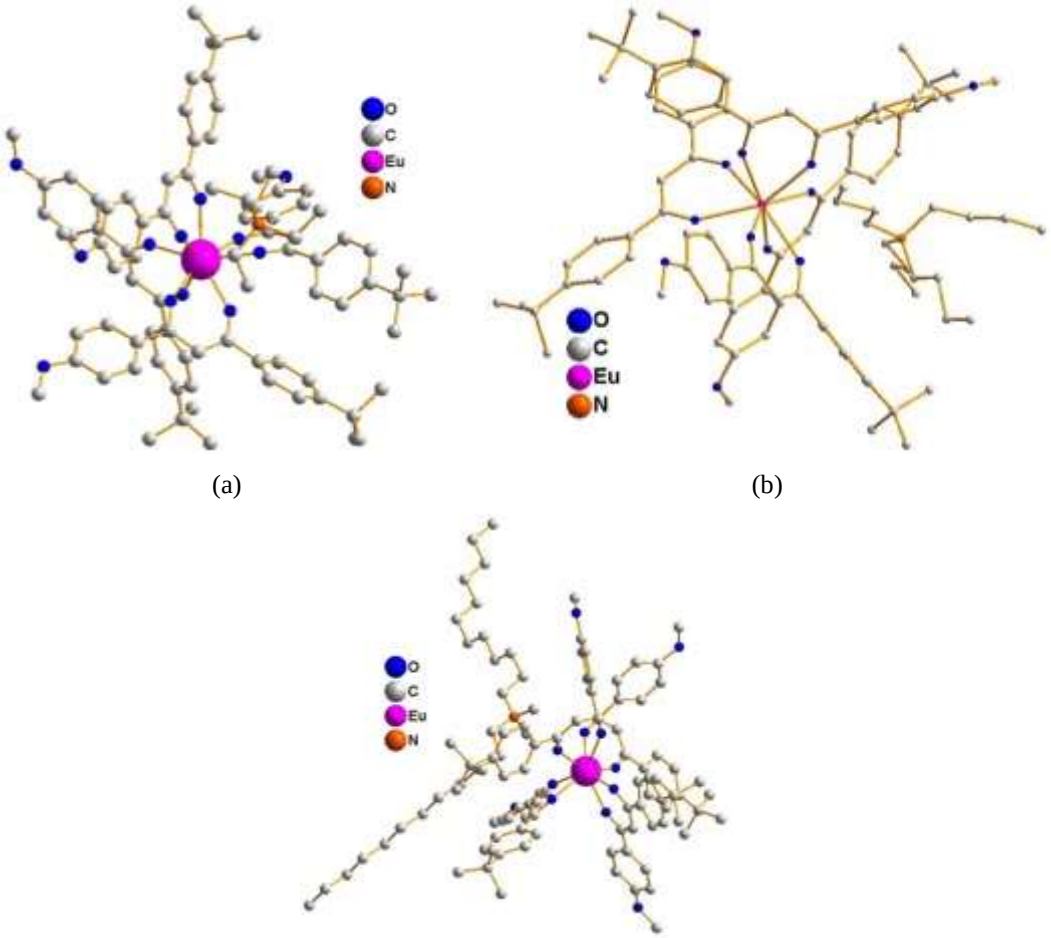

(a) (b)

(c)

Figure S7. Ground state geometry of the (a) $(N(C_2H_5)_4)^+[Eu(bmdm)_4]^-$; (b) $(N(C_4H_9)_4)^+[Eu(bmdm)_4]^-$ and (c) $(N(C_{12}H_{25})_2(CH_3)_2)^+[Eu(bmdm)_4]^-$ complexes obtained by the Sparkle/PM6.